

# Journal of Biomedical Optics

BiomedicalOptics.SPIEDigitalLibrary.org

## **Optical detection of middle ear infection using spectroscopic techniques: phantom experiments**

Hao Zhang  
Jing Huang  
Tianqi Li  
Sune Svanberg  
Katarina Svanberg

# Optical detection of middle ear infection using spectroscopic techniques: phantom experiments

Hao Zhang,<sup>a</sup> Jing Huang,<sup>a</sup> Tianqi Li,<sup>a</sup> Sune Svanberg,<sup>a,b</sup> and Katarina Svanberg<sup>a,b,\*</sup>

<sup>a</sup>South China Normal University, University City Campus, Center for Optical and Electromagnetic Research, Research Building 5, 510006 Guangzhou, China

<sup>b</sup>Lund University, Lund Laser Center, P.O. Box 118, SE-221 00 Lund, Sweden

**Abstract.** A noninvasive optical technique, which is based on a combination of reflectance spectroscopy and gas in scattering media absorption spectroscopy, is demonstrated. It has the potential to improve diagnostics of middle ear infections. An ear phantom prepared with a tissue cavity, which was covered with scattering material, was used for spectroscopic measurements. Diffuse reflectance spectra of the phantom eardrum were measured with a reflectance probe. The presence of oxygen and water vapor as well as gas exchange in the phantom cavity were studied with a specially designed fiber-optic probe for backscattering detection geometry. The results suggest that this method can be developed for improved clinical detection of middle ear infection. © 2015 Society of Photo-Optical Instrumentation Engineers (SPIE) [DOI: 10.1117/1.JBO.20.5.057001]

Keywords: middle ear infection; diffuse reflectance spectroscopy; gas in scattering media absorption spectroscopy; oxygen; water vapor; gas exchange.

Paper 140591RR received Sep. 16, 2014; accepted for publication Apr. 3, 2015; published online May 4, 2015.

## 1 Introduction

Middle ear infection (MEI), or otitis media, is a disease of the middle ear cavity and one of the most common infections in early childhood. One reason why children are more often affected as compared to adults is the fact that the ventilation channel of the middle ear, the Eustachian tube, is more horizontal at a young age and not downwards sloping into the nasal cavity (the nasopharynx). There are three principal types of ear infections—acute otitis media (AOM), otitis media with effusion (OME), and chronic otitis media with effusion (COME).<sup>1–4</sup> AOM is the most common of the ear infections. Most often, it is related to a common cold with an upper respiratory infection with blockage of the Eustachian tube and possible liquid aggregation in the middle ear cavity. It can cause sudden ear-ache and is associated by a cold or coughing. OME is an ear infection where fluid is trapped in the middle ear cavity without evident symptoms and may lead to deafness in severe cases. COME is the most destructive infection and happens when fluid stays in the middle ear cavity for a long time. Statistics show that more than three out of four young children have had at least one ear infection by the time they reach three years of age, and over one-third of the children will have recurring infections. An illustration of the human ear anatomy<sup>5</sup> is shown in Fig. 1, including an optical probe in position against the eardrum, the tympanic membrane (TM). The Eustachian tube plays a very important role in regulating the middle ear pressure and to drain fluid in the middle ear cavity.<sup>6</sup> Under normal conditions, the Eustachian tube is usually closed because of the pressure in the surrounding tissue, but it can open to allow air through thereby equalizing the pressure between the middle ear cavity and the atmosphere.<sup>7,8</sup> The tympanic cavity of a

healthy person is thus usually filled with air. Once infection occurs, the function of the Eustachian tube is impaired, and thereby the ventilation (i.e., the gas exchange) is blocked. As a result, the middle ear cavity is filled with liquids and pus, and in serious cases, the TM could rupture.<sup>1</sup>

A critical problem for otitis media diagnosis is that MEI mostly occurs in preschool children who cannot clearly describe the symptoms. Therefore, the parents may overlook the illness resulting in a delay in needed treatment. Further, communication problems may cause difficulties for the doctor to diagnose the infection. Myringitis is a further inflammatory condition which occurs in the TM, which is associated with viral or bacterial infections. The symptoms and signs of myringitis are very similar to those of AOM, so differentiating AOM from myringitis can be challenging.

A paramount clinical concern in MEI and myringitis management is the over-prescription of antibiotics, causing antibiotic resistance.<sup>9–11</sup> As an example, half of all antibiotics prescribed for children in the US are for ear infections, costing 2 billion USD/year,<sup>12</sup> in spite of the fact that antibiotics for middle ear problems due to very common viral infections have no therapeutic value. However, more stringent antibiotics recommendations are now beginning to be put in place in a few countries. It is clearly highly desirable to improve the diagnosis accuracy to guide correct treatment.

The diagnosis of otitis media is normally achieved by using an otoscope to visually examine the TM, which normally is translucent with a pale grayish appearance. An opaque red (or yellow) and bulging membrane may indicate an ear infection.<sup>13–16</sup> However, a visual assessment of the TM clearly contains subjective elements. Considering these problems regarding diagnosing otitis media and myringitis using an otoscope, and the alarming development of antibiotic resistance,

\*Address all correspondence to: Katarina Svanberg, E-mail: [katarina.svanberg@scnu.edu.cn](mailto:katarina.svanberg@scnu.edu.cn) or [katarina.svanberg@med.lu.se](mailto:katarina.svanberg@med.lu.se)

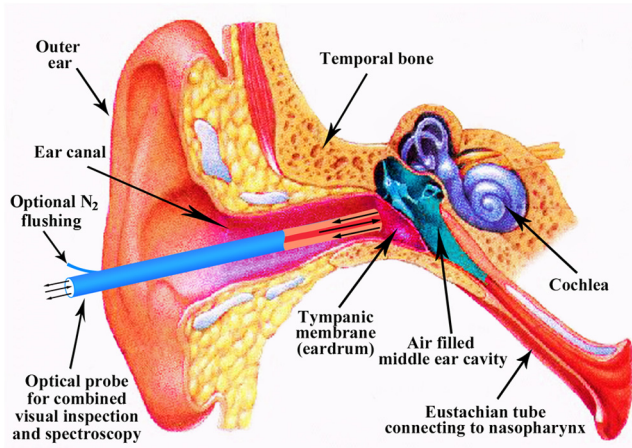


**Fig. 1** Anatomy of the human ear with the tympanic membrane, the middle ear cavity, and the Eustachian tube indicated. An optical probe for spectroscopy measurements, with means for nitrogen gas flushing to displace possible external residual oxygen and water vapor, is shown in place against the eardrum (adopted and modified from Ref. 5).

some additional accurate and easy-to-use diagnostic methods for a possible ear infection are essential and would be of great clinical value. A few not commonly used additional diagnosis methods include tympanometry<sup>17</sup> and acoustic reflectometry,<sup>18</sup> and have already been shown to improve the diagnosis accuracy.

Recently, some optical diagnostic methods have emerged. Sundberg et al.<sup>19</sup> used diffuse reflectance spectroscopy, basically for objectively evaluating the hemoglobin contents of the TM in children with and without otitis media. Optical coherence tomography (OCT)<sup>20</sup> based on low-coherence interferometry is a promising imaging technique with the feature of noninvasive detection and high resolution. Boppart et al.<sup>21</sup> used OCT combined with a fiber-based device to study the properties of the eardrum but also the possible effusion behind the eardrum related to OME. However, neither OCT nor diffuse reflectance spectroscopy can be used to detect impaired ventilation of the Eustachian tube.

As the middle ear normally is an air-filled cavity, and since this status changes with disease development, it would be valuable to monitor if gas is present, and if so, its composition. This is the main theme of the present paper and a method to pursue such studies is presented.

Gas in scattering media absorption spectroscopy (GSMAS)<sup>22,23</sup> is a noninvasive and easily implemented technique based on the fact that the absorption imprints of gases are about  $10^4$  times narrower than those of the surrounding solid materials. The method has been used for gas detection in the human sinuses and for monitoring the lungs of newborn infants.<sup>24–26</sup> GSMAS could, therefore, serve as a candidate technique for applications related to otitis media. Combined with diffuse reflectance spectroscopy, GSMAS has clear potential to be developed for providing improved diagnostic accuracy of otitis media and myringitis.

As described by Pogue and Patterson,<sup>27</sup> tissue-mimicking phantoms are extensively used for a number of purposes, e.g., for testing system designs, optimizing, and validating systems. This is also the case in the development of medical applications of GSMAS, where sinus phantoms<sup>28</sup> and neonatal

baby phantoms<sup>29</sup> have been employed. Along these lines, an ear phantom was constructed in the present work to explore the potential of the GSMAS technique, also in combination with diffuse reflectance spectroscopy, for the detection of MEI. Two physiological gases were studied; molecular oxygen was interrogated at 760 nm and water vapor at 937 nm. Actually, these two gases are the only two which can be readily studied, because of the necessity of the relevant spectral signatures to fall within the “tissue optical window,” 650 to 1300 nm, avoiding massive optical signal attenuation. Interestingly, these gases also happen to be of great interest to study for our purposes. Because of the special location of the measured gases, in the middle ear cavity, the common transmission detection geometry for GSMAS measurements is not applicable. In this study, backscattering detection geometry was adopted. For GSMAS in such detection geometry, the greatest challenge is that a large amount of light returns to the detector via the solid tissue and without passing the underlying gases. Here, a special fiber-optic probe was constructed to transmit and collect the light. The oxygen signal can be used to determine the oxygen content in the cavity and slow gas exchange through the Eustachian tube. The water vapor signal can be used to assess the volume of the cavity but can also be used as a reference gas with known concentration to infer the unknown concentration of oxygen.<sup>24,25</sup> In addition, the phantom was flushed with pure nitrogen and oxygen, followed by making a small orifice, and the return to equilibrium with normal gas composition was studied. In this way, we could clearly demonstrate that the recorded signals were indeed derived from the gas on the other side of the membrane and that oxygen normalization to water vapor is possible. In contrast to the case of human sinus cavities, where ventilation normally is fast,<sup>24</sup> gas exchange in the tympanic cavity of the middle ear through the Eustachian tube is quite slow and could be fully impaired in case of infection. Thus, the middle ear ventilation is not likely to be assessable for study over clinically realistic time spans. In addition to our middle ear gas studies, we demonstrated diffuse reflectance spectroscopy to objectively investigate, e.g., the hemoglobin change of the TM related to ear infections through analyzing the absorption spectra of this molecule, which has peaks at about 540 and 580 nm. The latter type of diagnostics has been very convincingly pursued by Sundberg et al.,<sup>19</sup> and we now explore the possibilities for a combined spectroscopic approach to improve the diagnostic accuracy of otitis media.

## 2 Materials and Methods

### 2.1 Phantom Preparation

The middle ear phantom was constructed with an enclosed tissue cavity formed from a fish swimming bladder, which was used as the “middle ear cavity.” The total volume of the cavity was about 2 mL, which is in close proximity to the volume of a real human tympanic cavity (1 to 2 mL). The tissue-like material (with regard to scattering properties) surrounding the cavity was made from a mixture of water (89%), gelatin (10%), and TiO<sub>2</sub> (1%). The detailed fabricating process of the phantom was performed as illustrated in Fig. 2. First, gelatin was added to water in a small glass beaker, which was placed in a larger water-filled beaker for heating [Fig. 2(a)]. Considering that the melting point of gelatin is at about 35°C, the temperature was set at 50°C.<sup>30</sup> The solution was stirred until the gelatin was completely dissolved and the solution appeared almost transparent. Then

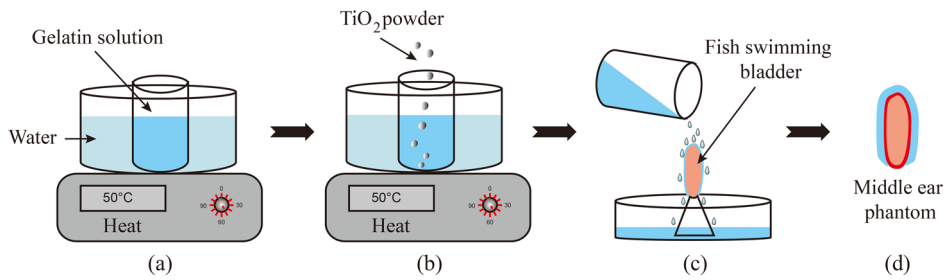


**Fig. 2** Illustration of the fabricating procedure of the middle ear phantom. (a) The different steps include the heating process for melting the gelatin, (b) adding the  $\text{TiO}_2$  powder, and (c) successively building up the scattering material around the phantom by pouring the dissolved solution are shown, (d) The ear phantom with a 3-mm thick tissue-like light-scattering layer is shown where a 10-mm diameter uncoated area (bottom) was left to mimic the eardrum.

$\text{TiO}_2$  was added to the solution which was maintained at a temperature of  $50^\circ\text{C}$  [Fig. 2(b)]. Finally, an expanded fresh fish swimming bladder was put into a holder, and the solution was poured over it [Fig. 2(c)]. Partial solidification occurred at room temperature, and the process was repeated until the covering layer was about 3-mm thick [Fig. 2(d)].

### 2.2 Construction of the Fiber-Optic Probe

The fiber-optic probe used for GASMAS measurements was constructed with nine optical fibers, where one fiber with the

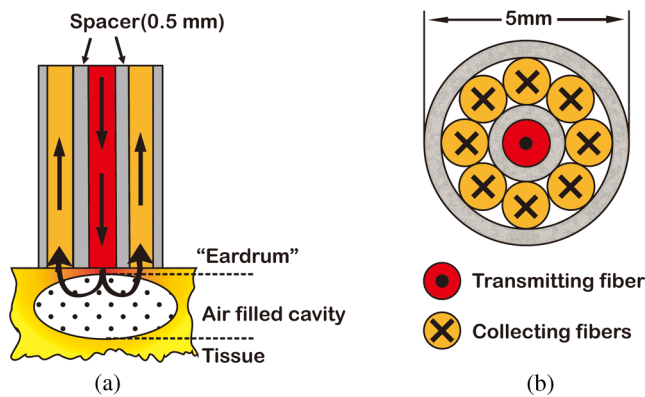


**Fig. 3** Schematic drawings of the fiber-optic probe tip, showing (a) a longitudinal view and (b) a transverse view of the probe used for GASMAS measurements of free gas located behind the “eardrum” in a back-scattering geometry.

core diameter of  $600\ \mu\text{m}$  was used as transmitting fiber and the other fibers with a core diameter of  $400\ \mu\text{m}$  were used as collecting fibers, as displayed in Fig. 3. The fibers were manufactured by Nanjing Chun Hui Science & Technology Industrial Co., Ltd., China. All the fibers were coated with plastic and had a total diameter of 1 mm. Since reflected light without any gas absorption can dilute the signal, the distance between the transmitting fiber and the collecting fibers must be optimized to enhance the fraction of light which has passed through the gas-filled space behind the eardrum, while observing the constraint that the total diameter of the probe must be compatible with the external auditory canal diameter. The considerations follow the procedures discussed for the case of sinus cavity monitoring in backscattering.<sup>31</sup> After extensive testing, a 0.5-mm spacing distance between the coated transmitting and collecting fibers resulting in a total probe diameter of about 5 mm was selected for optimized measurements (see Fig. 3).

### 2.3 Experimental Setup

A schematic drawing of the GASMAS setup used for gas detection is shown in Fig. 4(a). Two diode lasers (LD-0760-0100 and LD-0937-0100, Toptica, Munich, Germany) operating at the oxygen absorption line at  $760.445\ \text{nm}$  and the water vapor absorption line at  $937.405\ \text{nm}$ , respectively, were used as light sources. Laser current and temperature controllers (LCD 201C and TED 200C, Thorlabs, Newton, New Jersey) were used to control the drive current and the temperature of the diode lasers. The controlling current of the laser was superimposed with a

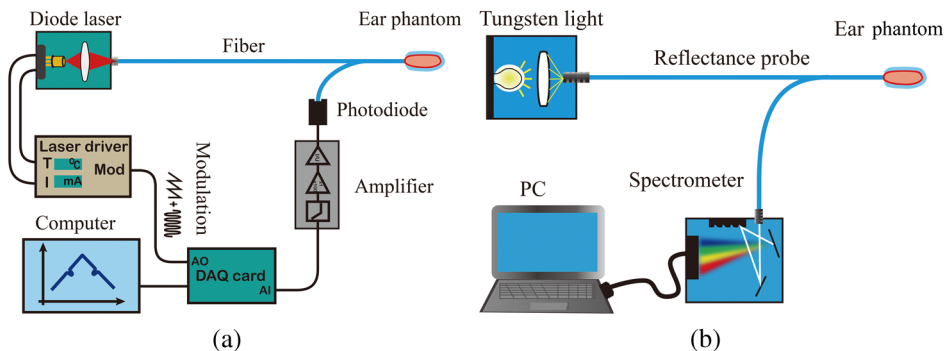


**Fig. 4** Schematic drawing of the two set-ups used for the measurements on the ear phantom. (a) GASMAS measurements in a backscattering geometry of gas behind the “eardrum” and (b) diffuse reflectance measurements on the “eardrum.”

5-Hz ramp wave as well as with a 10,295 Hz sinusoidal wave for oxygen measurement and a 9015 Hz sinusoidal wave for water vapor measurement, which were created by a LabVIEW program. Among these superimposed signals, the ramp wave was utilized to scan the absorption line and the sinusoidal wave was used to modulate the laser to acquire the harmonic signals for software-based lock-in detection. The modulated laser light was injected into the ear phantom through the transmitting fiber and the backscattered light received by the collecting fibers [see Fig. 4(a)] was detected by a photodiode (S3204-08, Hamamatsu Photonics, Hamamatsu, Shizuoka, Japan). The current signal from the photodiode was converted to a voltage signal and then amplified by a variable gain low-noise current amplifier (DLPCA-200, Femto, Berlin, Germany) before being recorded by the input channel of the data acquisition (DAQ) card (NI6120, National Instruments, Austin, Texas).

The experimental setup for reflectance spectral measurements is illustrated in Fig. 4(b). Broadband light from a tungsten lamp was transmitted to the ear phantom through a 400- $\mu\text{m}$  core diameter fiber. The reflected light from the surface of the “eardrum” was captured with a reflectance probe (Ocean Optics, Dunedin, Florida) and then detected by a portable spectrometer (USB4000, Ocean Optics). The obtained data were analyzed by the Ocean Optics SpectraSuite software and transformed to the spectral profile. It can be seen from Fig. 4(b) that the reflectance probe in its present implementation is different from the fiber-optic probe used for GASMAS measurements. The reflectance probe was constructed with  $13 \times 400 \mu\text{m}$  fibers where one was used as transmitting fiber and the rest of the fibers were used as collecting fibers, and all the fibers were integrated in a compact way. Before the measurements, the system was calibrated for intensity using a calibration lamp (IES 1000, Labsphere, North Sutton, New Hampshire) and for wavelength with a low-pressure mercury lamp.

## 2.4 Data Analysis

The recorded GASMAS data were analyzed with digital lock-in techniques to get the second harmonic ( $2f$ ) signal. Then the  $2f$  signal was normalized by dividing it with a direct signal (the signal without gas absorption) to achieve the normalized  $2f$  signal, which is insensitive to the amount of light detected by a photodiode. A detailed discussion of the digital lock-in detection and normalization is given in Ref. 32. Considering the influence of optical interference fringes which come from optical elements in the light path, a small vibration motor was used to mechanically modulate and thereby shift the positions of possible etalon fringes to minimize spurious interference.<sup>33</sup> Minute remaining modulations in the detected light could otherwise mimic absorption lines with similar line width. In this study, a matched version of the reference signal as measured by sending the laser directly to the detector was subtracted from the sample signal obtained from the beam which passed the sample to yield a so-called balanced detection signal.<sup>34</sup> The matching intensity is found by fitting the reference signal to the sample signal at frequency regions outside the expected oxygen imprint. A sloping signal background could in this way be accurately removed.

Due to the strong scattering of the light travelling in tissue, the path length is unknown, and the gas concentration is not easy to be estimated by the Beer–Lambert law. The obtained  $2f$  signal was fitted to a reference signal which was measured over

an ambient atmosphere distance, and a so-called equivalent mean path length,  $L_{\text{eq}}$ , could be obtained, corresponding to the path length that the light would travel in ambient air to get the same oxygen or water vapor absorption imprint. The  $L_{\text{eq}}$  can be described by the equation

$$L_{\text{eq}} \times C_{\text{air}} = \bar{L}_{\text{sample}} \times C_{\text{sample}}, \quad (1)$$

where  $C_{\text{air}}$  is the gas concentration in ambient air,  $\bar{L}_{\text{sample}}$  is the mean path length that light travels in the sample, and  $C_{\text{sample}}$  is the gas concentration in the sample. As can be seen from Eq. (1),  $L_{\text{eq}}$  is proportional to the gas concentration in the sample, so it can be used to assess the desired gas content.

## 3 Results and Discussion

### 3.1 GASMAS Measurements

Before performing the measurements, the ear phantom was perforated to obtain a small orifice and then left in ambient conditions for 24 h. Thus, we mimic the condition of a tympanic cavity in which the gas composition is the same as that of the atmospheric air as regulated by the Eustachian tube. Measurements of oxygen and water vapor were performed sequentially with the probe positioned against the small part of the fish-bladder wall, which was not covered with scattering material (our “eardrum”). Molecular oxygen was measured first, followed directly by water vapor measurement with the same procedure. All the measurements were performed in ambient room conditions with a temperature of about 23°C and a relative humidity of about 60%. During the measurements, each recorded signal was averaged for about 1 min. A typical recorded  $2f$  oxygen signal from the measurement on the ear phantom and the fitted curve from the measurement on a 1100 mm path of ambient air are shown in Fig. 5(a). A water vapor signal from the ear phantom measurement and the fitted curve from ambient air are shown in Fig. 5(b). These signals correspond to an absorption fraction of about  $1.8 \times 10^{-4}$  and  $1.3 \times 10^{-3}$  for oxygen and water vapor, respectively.

Interpreted from these results, GASMAS shows a good performance using the special probe in a backscattering detection geometry, even though the measured oxygen signal is intrinsically weak. Studies of gas exchange in the phantom were performed for assuring that the recorded GASMAS signals were in fact due to the gas behind the membrane. Now, the cavity was flushed with pure oxygen or nitrogen through the small orifice until the cavity was enriched with oxygen or nitrogen, and then the orifice was sealed. Due to the liquid water in the surrounding tissue, a humidity of about 100% and a temperature close to 37°C is expected in the real human tympanic cavity. Therefore, some liquid water was injected into the phantom cavity to achieve 100% humidity in the middle ear phantom cavity before the water vapor measurements. Continued measurements were then performed for each gas, integrating the signal and reading out the result intermittently, to create a recording of gas content as a function of time. The orifice was opened after measurements for 5 min (as indicated in the figures) in order to study subsequent gas exchange. The experimental results are shown in Fig. 6.

As can be observed in Fig. 6(a), the measured oxygen  $L_{\text{eq}}$  reaches a high value after flushing with oxygen and stays stable. Then, it decreases gradually to the ambient air equilibrium of 21% oxygen after opening the orifice of the cavity. We note

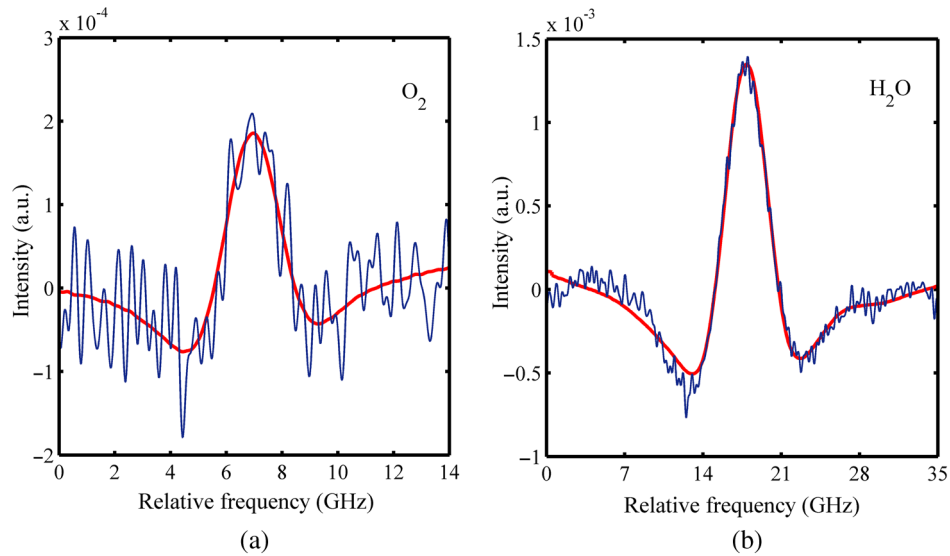


**Fig. 5** (a) Typical measured  $2f$  signal of oxygen and (b) water vapor obtained on the ear phantom using backscattering detection. The signals were integrated over 60 s.

that the oxygen flushing resulted in an initial concentration of about 60%. Similarly, Fig. 6(b) shows that a low signal due to residual oxygen (about 9%) after the flushing with nitrogen is observed, followed by an increase to ambient 21% on the re-invasion of ambient air through the open orifice. Thus, a wide range of oxygen concentrations could be recorded. As indicated with the fitted red curves in Fig. 6, an exponential function with a time constant of about 3 min can be fitted to the experimental data to describe the oxygen gas exchange. We note that middle ear ventilation through the Eustachian tube would in reality be much slower, and in most cases, impractical to monitor. In this study, the ventilation rate of the ear phantom is dependent on

the size of the small puncture, and the goal for the measurements of gas exchange is only to demonstrate that the measured signals come from the gas in the tympanic cavity and not due to any spurious gas absorption in the measurement system. A different behavior is observed when comparing Figs. 6(a) and 6(b) with Figs. 6(c) and 6(d), which are the results for the water vapor signal with oxygen and nitrogen flushing, respectively. The  $L_{eq}$  values have no noticeable change after flushing, which can be explained by the establishment of 100% saturated water vapor conditions in the liquid water-containing cavity almost immediately after flushing of the cavity with dry gas. This fact also proves that the water vapor can be used as a reference

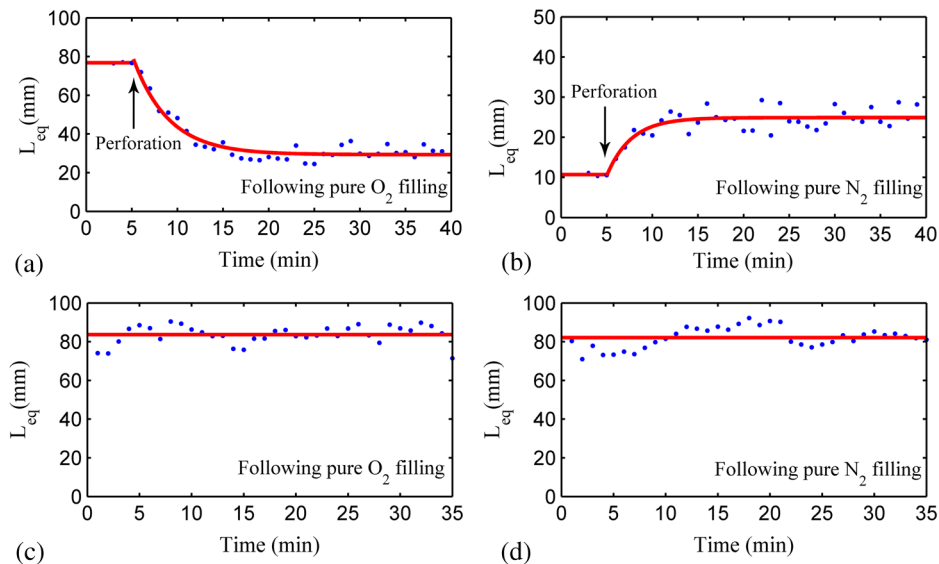


**Fig. 6** Studies for gas exchange after perforation of the ear phantom, with the measured  $L_{eq}$  value given as a function of time following (a and c) oxygen and (b and d) nitrogen flushing of the cavity. The purpose of these measurements is to show that the recorded gas signals are indeed due to gas on the other side of the membrane (inside the cavity), and not due to spurious gas, and that the water vapor signal, being stable, can serve for normalization purposes. Each data point corresponds to 60 s of signal integration.

gas of known concentration to estimate by normalizing the true concentration of the biologically active gas oxygen in the tympanic cavity, as described in Ref. 24. This can then be achieved even if the optical path length is unknown due to scattering, and calibration by ambient concentration oxygen is not available. In addition, the time evolution of the water vapor signal also shows the stability of measurement system. As a matter of fact, it can also be seen from Fig. 6 that the experimental data exhibit some fluctuations during the continuous measurements. This could be the result of still uncompensated residual optical interference fringes, affecting the fitting procedure.

### 3.2 Reflectance Spectral Measurements

Ear infection causes the eardrum to change in color from grayish to reddish, and in serious cases, it may lead to a ruptured eardrum. In this study, some human blood was used to cover the surface of the eardrum phantom to simulate an infected eardrum. The measured reflectance spectra from the “normal” (black curve) and the “infected” (red curve) eardrum phantom are shown in Fig. 7. It can be seen that two prominent absorption peaks appear at about 540 and 580 nm, which are the blood absorption imprints. In addition, another peak appears at about 630 nm, which could be the absorption imprint of methemoglobin (Mhb) in the fish swimming bladder.<sup>35,36</sup> For the reflectance spectra of a real human eardrum, the last absorption peak does not exist, so this phenomenon can be ignored in the present study. When the ear suffers from infection, the eardrum becomes red and possibly dilates. The reflectance spectrum from the “infected” eardrum clearly has some differences from that of the normal one, just as the curves indicated in Fig. 7, where the typical two blood absorption peaks are much larger for the “infected” eardrum.

In order to quantify the erythema of the TM from acquired diffuse reflectance spectra, an erythema index can be defined to quantify the reddening. Such an index was proposed by Feather et al.<sup>37</sup> It is evaluated using the blood absorption imprint in the diffuse reflectance and is linearly dependent on the hemoglobin

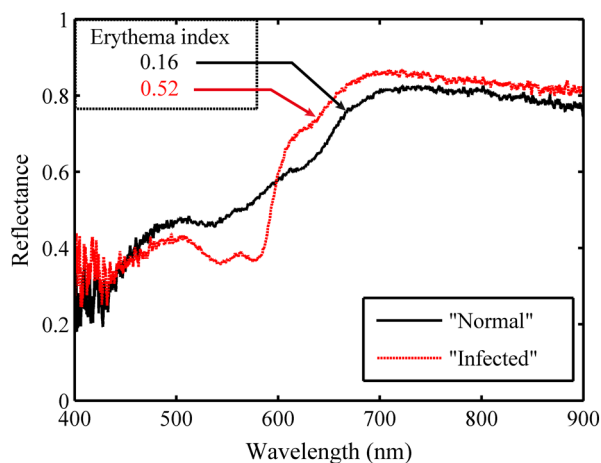


**Fig. 7** Reflectance spectra of the membrane in the ear phantom measured by diffuse reflectance spectroscopy. When human blood is added to the fish-bladder wall to mimic a reddened eardrum, the typical hemoglobin absorption imprints at 540 and 580 nm are clearly seen. The differences in spectral shape can be quantified by using an “erythema index,” which in this case differs by a factor of 3.

concentration. Index values from the two recorded spectra are indicated in the figure as calculated with a formula, slightly modified from Feather et al.<sup>37</sup> We note that the ratio of the index values is about 3, illustrating how the difference in spectral shape can lead to a quantified considerable contrast between normal and diseased conditions. Clearly, the diffuse reflectance spectrum gives more objective and quantitative information than what is possible with human eye inspection, as noted by Sundberg et al.<sup>19</sup>

## 4 Conclusion and Outlook

The results obtained in the middle ear phantom measurements show that the GASMAS technique has the potential to study the gas content in the human middle ear cavity, and in particular to quantify the oxygen content by normalization to the known content of water vapor, as demonstrated in work on human sinuses.<sup>24</sup> The possible presence of an air-pocket between the optical probe head and the eardrum in a real clinical measurement could result in spurious gas signals. It could be eliminated by gently flushing this space with nitrogen, as indicated in Fig. 1. Such a procedure is frequently employed in other GASMAS projects, especially in noninvasive inspection of head-space gas on food containers, where perfect probe contact cannot be ensured in measurements on moving packages on a conveyor belt.<sup>38</sup> Another more interesting aspect of nitrogen flushing is that the ventilation of the cavity through the Eustachian tube can, in principle, be studied by harmless nitrogen flushing of the nasal cavity causing displacement of oxygen in the connected cavities, as shown for sinuses in Ref. 24. However, as we have noted, the much slower gas exchange for the middle ear would render such a procedure clinically impractical, leaving this possibility for research purposes, e.g., for objectively assessing the efficacy of anticongestion medication.

As earlier demonstrated, e.g., in Ref. 19, diffuse reflectance spectroscopy provides the possibility to more objectively study redness and hemoglobin changes of the human eardrum. Multivariate spectral decomposition can be a powerful tool for studies of minor spectral changes, which we have explored extensively in other contexts (see, e.g., Refs 39 and 40). This might objectively, through the translucent eardrum, reveal the presence of yellow pus or other fluid anomalies in the middle ear cavity caused by infection. The conventional diagnosis of MEI is to study the eardrum with otoscopy which is only based on visual inspection. The spectroscopic techniques discussed can provide additional valuable information for the detection of MEI. Our study suggests that a combination of the two methods which we have explored could make the detection of MEI and myringitis more objective and reliable. The total measurement time in an optimized system could be reduced to <10 s. In particular, we expect that the capability of GASMAS to objectively assess the presence of free gas behind the eardrum and also to provide a direct measurement of the oxygen concentration in the cavity, determining aerobic or non-aerobic conditions, would add substantially in the management of otitis media.

Although the measurements were performed on an ear phantom, not a real human middle ear, the results suggest that a viable method for the diagnosis of MEI can be developed. We are now constructing an instrument where GASMAS can be fully integrated with diffuse reflectance spectroscopy to provide objective and improved clinical diagnosis of MEI.

Measurements on volunteers are planned. In the present work, sequential measurements are performed on oxygen and water vapor. These two types of measurements could be performed simultaneously with the same detector and different modulation frequencies, as utilized in our previously described sinus monitoring system.<sup>25</sup> A compact adapted system, incorporating GASMAS, diffuse reflectance spectroscopy, and visual inspection, along the lines indicated in Fig. 1, for deployment in clinical trials on patients, is the final goal of our ongoing project.

### Acknowledgments

The authors gratefully acknowledge the support of Prof. Sailing He. This work was financially supported by a Guangdong Province Innovation Research Team Program (No. 201001D0104799318).

### References

- C. D. Bluestone and J. O. Klein, *Otitis Media in Infants and Children*, 4th ed., PMPH-USA, Ltd., Shelton (2007).
- L. M. T. Dicks, H. Knoetze, and C.A. van Reenen, "Otitis media: a review, with a focus on alternative treatments," *Probiotics Antimicrob. Proteins* **1**(1), 45–49 (2009).
- S. Maxson and T. Yamauchi, "Acute otitis media," *Pediatrics Rev.* **17**(6), 191–195 (1996).
- H. Kubba, J. P. Pearson, and J. P. Birchall, "The aetiology of otitis media with effusion: a review," *Clin. Otolaryngol. Allied Sci.* **25**(3), 181–194 (2000).
- S. Evans, "How does your ear work?," <http://drsetheevans.com/2014/01/27/how-does-your-ear-work/>.
- J. L. Dornhoffer et al., *A Practical Guide to the Eustachian Tube*, Springer, Berlin (2014).
- S. Ingelstedt and B. Jonson, "Mechanisms of the gas exchange in the normal human middle ear," *Acta Oto-Laryngol.* **63**(S224), 452–461 (1967).
- A. Elner, "Normal gas exchange in the human middle ear," *Ann. Otol. Rhinol. Laryngol.* **85**(2 Suppl 25 Pt 2), 161–164 (1975).
- A. J. Leach, P. S. Morris, and J. Amanda, "Antibiotics for the prevention of acute and chronic suppurative otitis media in children," *Cochrane Database Syst. Rev.* **4**, CD004401 (2006).
- G. H. McCracken, "Treatment of acute otitis media in an era of increasing microbial resistance," *Pediatr. Infect. Dis. J.* **17**(6), 576–579 (1998).
- S. F. Dowell et al., "Acute otitis media: management and surveillance in an era of pneumococcal resistance - a report from the drug-resistant Streptococcus pneumoniae Therapeutic Working Group," *Pediatr. Infect. Dis. J.* **18**(1), 1–9 (1999).
- T. R. Coker et al., "Diagnosis, microbial epidemiology, and antibiotic treatment of acute otitis media in children: a systematic review," *J. Am. Med. Assoc.* **304**(19), 2161–2169 (2010).
- K. Ramakrishnan, R. A. Sparks, and W. E. Berryhill, "Diagnosis and treatment of otitis media," *Am. Fam. Phys.* **76**(11), 1650–1658 (2007).
- S. L. Block and C. J. Harrison, *Diagnosis and Management of Acute Otitis Media*, 3rd ed., Professional Communications, Inc., West Islip, New York (2005).
- American Academy of Pediatrics, Subcommittee on Management of Acute Otitis Media, "Diagnosis and management of acute otitis media," *Pediatrics* **113**(5), 1451–1465 (2004).
- A. S. Lieberthal et al., "The diagnosis and management of acute otitis media," *Pediatrics* **131**(3), e964–e999 (2013).
- P. E. Brookhouser, "Use of tympanometry in office practice for diagnosis of otitis media," *Pediatr. Infect. Dis. J.* **17**(6), 544–551 (1998).
- S. L. Block et al., "Spectral gradient acoustic reflectometry for the detection of middle ear effusion by pediatricians and parents," *Pediatr. Infect. Dis. J.* **17**(6), 560–564 (1998).
- M. Sundberg et al., "Diffuse reflectance spectroscopy of the human tympanic membrane in otitis media," *Physiol. Meas.* **25**(6), 1473–1483 (2004).
- A. F. Fercher, "Optical coherence tomography," *J. Biomed. Opt.* **1**(2), 157–163 (1996).
- S. A. Boppart and Chuanwu Xi, "Device and method for imaging the ear using optical coherence tomography," U.S. Patent No. 20090185191A1 (2009).
- M. Sjöholm et al., "Analysis of gas dispersed in scattering media," *Opt. Lett.* **26**(1), 16–18 (2001).
- S. Svanberg, "Gas in scattering media absorption spectroscopy – from basic studies to biomedical applications," *Lasers Photonics Rev.* **7**(5), 779–796 (2013).
- L. Persson et al., "Gas monitoring in human sinuses using tunable diode laser spectroscopy," *J. Biomed. Opt.* **12**(5), 054001 (2007).
- M. Lewander et al., "Clinical study assessing information of the maxillary and frontal sinuses using diode laser gas spectroscopy and correlating it with CT," *Rhinology* **50**, 26–32 (2011).
- P. Lundin et al., "Non-invasive monitoring of gas in the lungs and intestines of newborn infants using diode lasers: feasibility study," *J. Biomed. Opt.* **18**(12), 127005 (2013).
- B. W. Pogue and M. S. Patterson, "Review of tissue simulating phantom for optical spectroscopy, imaging and dosimetry," *J. Biomed. Opt.* **11**(4), 041102 (2006).
- L. Persson, K. Svanberg, and S. Svanberg, "On the potential for human sinus cavity diagnostics using diode laser gas spectroscopy," *Appl. Phys. B* **82**(2), 313–317 (2006).
- M. Lewander et al., "Non-intrusive gas monitoring in neonatal lungs using diode laser spectroscopy: feasibility study," *J. Biomed. Opt.* **16**(12), 127002 (2011).
- P. Lai, X. Xu, and L. Wang, "Dependence of optical scattering from intralipid in gelatin-gel based tissue-mimicking phantoms on mixing temperature and time," *J. Biomed. Opt.* **19**(3), 035002 (2014).
- L. Persson et al., "Monte Carlo simulations related to gas-based optical diagnosis of human sinusitis," *J. Biomed. Opt.* **12**(5), 054002 (2007).
- M. Lewander et al., "Clinical system for non-invasive in situ monitoring of gases in the human paranasal sinuses," *Opt. Express* **17**(13), 10849–10863 (2009).
- T. Svensson et al., "High sensitivity gas spectroscopy of porous, highly scattering solids," *Opt. Lett.* **33**, 80–82 (2008).
- L. Persson et al., "Approach to optical interference fringe reduction in diode-laser-based absorption spectroscopy," *Appl. Phys. B* **87**(3), 523–530 (2007).
- D. R. Buhler, "Studies on fish hemoglobins: chinook salmon and rainbow trout," *J. Biol. Chem.* **238**(5), 1665–1674 (1963).
- J. A. Lacey and K. J. Rodnick, "Important considerations for methaemoglobin measurement in fish blood: assay choice and storage conditions," *J. Fish Biol.* **60**(5), 1155–1169 (2002).
- J. W. Feather et al., "A portable scanning reflectance spectrophotometer using visible wavelengths for the rapid measurement of skin pigments," *Phys. Med. Biol.* **34**(7), 807–820 (1989).
- M. Lewander et al., "Non-intrusive measurements of headspace gas composition in liquid food packages made of translucent materials," *Packaging Technol. Sci.* **24**(5), 271–280 (2011).
- A. Runemark et al., "Rare events in remote dark field spectroscopy: An ecological case study of insects," *IEEE J. Sel. Top. Quantum Electron.* **18**(5), 1573–1582 (2012).
- M. Brydegaard et al., "Complete parameterization of temporally and spectrally resolved laser induced fluorescence data with applications in bio-photonics," *Chemometrics Intell. Lab. Syst.* **142**, 95–106 (2015).

**Hao Zhang** received his bachelor's degree in physics from the East China Institute of Technology, Nanchang, in 2011. His major field was optical engineering. He is now a PhD student at the Center for Optical and Electromagnetic Research at South China Normal University, Guangzhou. His current research interests concern applications of laser spectroscopy to the biophotonics field.

**Jing Huang** received her bachelor's degree at the Guangdong University of Technology in Guangzhou in 2012. She is now a master's student at the Center for Optical and Electromagnetic Research at South China Normal University, Guangzhou. Her research interests include laser spectroscopy applied to food safety and biomedical topics.

**Tianqi Li** received her bachelor's degree in applied physics at the Hefei University of Technology in 2013. She is now a master's student

at the Center for Optical and Electromagnetic Research at South China Normal University, Guangzhou. Her research interests include laser spectroscopy applied to food safety and biomedical topics.

**Sune Svanberg** obtained his PhD degree from the University of Gothenburg in 1972, and since 1980, he has been a professor of physics at Lund University, Lund, Sweden. For 30 years, he was head of the Atomic Physics Division, and for 20 years he was director of the Lund Laser Center. Since 2011, he has also been a distinguished professor at the South China Normal University,

Guangzhou. His research interests include laser spectroscopic applications to the environmental, food safety, and biomedical fields.

**Katarina Svanberg** obtained her PhD degree from Lund University in 1989 and is a professor at the Department of Oncology, Lund University Hospital, where she has been active as chief consultant for 25 years. Since 2011, she has also been a distinguished professor at South China Normal University, Guangzhou. Her research interests include applications of laser spectroscopy to the biomedical and biophotonics fields.